JOURNAL OF PROPULSION AND POWER
Vol. 12, No. 2, March–April 1996

Holography Experiments in a Dense High-Speed Impinging Jet Spray

B. S. Kang* and D. Poulikakos†
University of Illinois at Chicago, Chicago, Illinois 60607-7022

In this article an experimental study of the fluid dynamics of a spray created by two high-speed impinging jets is presented. Utilizing a novel two-reference-beam double-pulse holographic technique, the effects of the impingement angle, liquid jet velocity, orifice diameter, and liquid properties on the atomization process were investigated. Visualization of the overall spray pattern and measurements of the size and velocity of the droplets were performed. The overall spray pattern clearly revealed the inherent wave nature in the disintegration process for this type of atomization. Smaller droplets were generated more rapidly, in a shorter distance from the impingement point, with larger impingement angles, higher jet velocities, and smaller orifice diameters. Surface tension played an important role in the droplet size without any noticeable effect on the spray pattern, whereas viscosity affected the structure without any significant effect on the droplet size. The droplet velocities were not affected markedly by the liquid properties. The superiority of the universal root-normal distribution to the Rosin–Rammler distribution was proved in the great majority of cases tested.

Nomenclature

D = diameter
D_j = orifice diameter, Fig. 1
D_{MMD} = mass median diameter
D_{10} = length-mean diameter
D_{32} = Sauter-mean diameter
r = radial distance from the impinging point, Fig. 1
R = liquid jet radius
Re_j = Reynolds number of liquid jet
V = velocity
V_j = velocity of liquid jet
V_m = magnitude of velocity vector of droplet
We_j = Weber number of liquid jet
x = horizontal coordinate from impinging point, Fig. 1
y = vertical coordinate from impinging point, Fig. 1
θ = half of the axis-to-axis angle of the impinging jets
μ = viscosity of liquid
ρ = density of air
ρ_l = density of liquid
σ = surface tension of liquid

I. Introduction

IMPINGING-JET injectors are commonly used in liquid propellant rocket engines.[1,2] The liquid propellants (the fuel and oxidizer) are injected through a number of separate small holes in such a manner that they impinge upon each other. Combustion instabilities in rocket engines are characterized by sustained pressure oscillations. The origin of the instabilities appears to be related to the atomization and mixing processes of the propellants. Photographs of the spray formed by two impinging jets show the periodic nature of the atomization process.[3,4] Groups of droplets resulting from the breakup of liquid ligaments give the impression of waves originating from the impingement point. The mechanisms that initiate and sustain these phenomena have not been disclosed satisfactorily.

As shown schematically in Fig. 1, two impinging high-speed jets form a small fan-shaped liquid sheet around the impingement point. This liquid sheet quickly disintegrates into unstable arc-shaped liquid ligaments that contract themselves by surface tension and finally break into droplets. The spray characteristics depend on V_j, D_j, 2θ, the conditions of the surroundings, and the physical properties of the liquid.

Studies on the spray characteristics of impinging-jet injectors started in the 1950s and 1960s and were focused on revealing the sheet breakup mechanisms and predicting the size distribution of droplets. Heidmann et al.[4] investigated the effects of orifice diameter, jet velocity, impingement angle, preimpingement length, and liquid properties (viscosity, surface tension) on the structure of the spray. The spatial characteristics of water sprays were investigated by Foster and Heidmann.[5,6] Dombrowski and Hooper[7] studied the mechanism of the disintegration of liquid sheets formed by two impinging laminar and turbulent jets. They contributed the mechanism to the formation of unstable waves of aerodynamic or hydrodynamic origin. Huang[8] investigated the breakup mechanism of

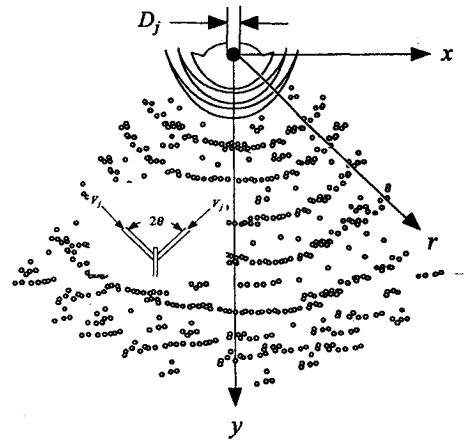

Fig. 1 Schematic diagram of a spray formed by two high-speed impinging jets. The insert in this figure shows a side view of the impingement region.

Received March 25, 1995; revision received Oct. 15, 1995; accepted for publication Nov. 3, 1995.

*Graduate Research Assistant, Department of Mechanical Engineering; currently Senior Scientist, Korean Academy of Industrial Technology, 152-020, 271-36, Karibong-Dong, Kuro-Ku, Seoul, Republic of Korea.

†Professor, Department of Mechanical Engineering; currently at Swiss Federal Institute of Technology, CH-8092, Zurich, Switzerland.

axisymmetric liquid sheets formed by the impingement of two coaxial water jets. He reported three breakup regimes depending on the Weber number of the liquid jet. Recent research conducted by Anderson et al.[9] focused on the characteristics of the spray created by two turbulent impinging jets. The mean drop diameters decreased with an increase in the jet velocity and impingement angle. The mean drop velocities were almost equal to the jet velocity, regardless of the impingement angle and measured position. Ryan et al.[11] extended Anderson et al.'s work[9] to investigate the effects of the jet conditions (laminar vs turbulent), orifice diameter, impingement angle, and jet velocity on the atomization of impinging liquid jets. The experimental results contrasting the laminar and turbulent jet conditions demonstrated that the jet conditions had a significant effect on the atomization process. They also modeled the disintegration of sheets formed by two impinging liquid jets using two existing theories: 1) a stationary antisymmetric wave-based theory for low Weber numbers[12] and 2) a linear stability-based theory for high Weber numbers.[9] Vassallo et al.[13] investigated the spray characteristics of two and four impinging-jet injectors using phase doppler particle analysis.

This study reports the main results of an experimental investigation, based on two-reference double-pulse holography, for the visualization of the spray structure as well as the measurement on the size and velocity of the liquid droplets. The study focuses on the dense spray region where liquid elements are rather large and nonspherical. The experiments involved two nonevaporating impinging jets injected into still air at atmospheric pressure. The effect of several factors on the spray characteristics was examined using water, ethanol, and three glycerol solutions as test liquids. Theoretical predictions on the mean droplet size were also attempted and tested against the experimental results. The frequently used droplet size distributions were compared with the experimental results to validate their application to experimental data.

II. Experiments

A. Impinging Jet Apparatus

The experimental apparatus for two impinging jets (not shown for brevity) is described in detail elsewhere.[14] Herein, only a brief description is contained. High-pressure N_2 gas was used for pressurizing a liquid reservoir. The liquid flow from a flow meter passed through an on–off valve and was divided into two identical branches for the individual liquid jets. Precision-bore glass tubes were used as impinging jet injectors. The i.d. of the tubes in this study were 1.016 and 1.534 mm. The length of the tubes was 0.152 m. A 50.8-mm-long, 6.35-mm-o.d. copper tube bonded at one end of each glass tube was connected to the liquid-supplying plastic tube. The entry to the glass tube was smoothly contoured to maintain laminar flow conditions at the injector exit. The laminar flow condition up to the Reynolds number of about 1×10^4 was indicated by visual observations such as no ruffling of liquid jet boundaries and a clear glassy appearance of the jets. Each injector was mounted on a high-precision rotation stage in a manner that allowed for fine tuning until a perfect liquid sheet normal to the liquid jet plane was obtained.[14] The impingement angle was adjusted accurately by the rotation stages. The falling liquid was collected into a cylindrical liquid tank.

B. Optical System for Hologram Recording

A novel technique was used for the recording of the holograms used for the velocity measurements. This technique allows for the separate reconstruction of the spray image obtained by different pulses of the light source, an advantage that greatly facilitates the image processing of the holograms, particularly in the dense spray region. Figure 2 shows the schematic layout of the holographic recording system. The light source is a ruby laser that can generate a 694-nm-wavelength, vertically polarized, 1-J output energy, either single- or double-pulse laser beam. The pulse interval was 50 μs (after a trial-and-error process). The short pulse duration (30 ns) assures the freezing of all moving liquid elements or droplets and the clarity of the resulting images. For the alignment of all optical components before firing the ruby laser, a He–Ne alignment laser that is mounted on the ruby laser box was used.

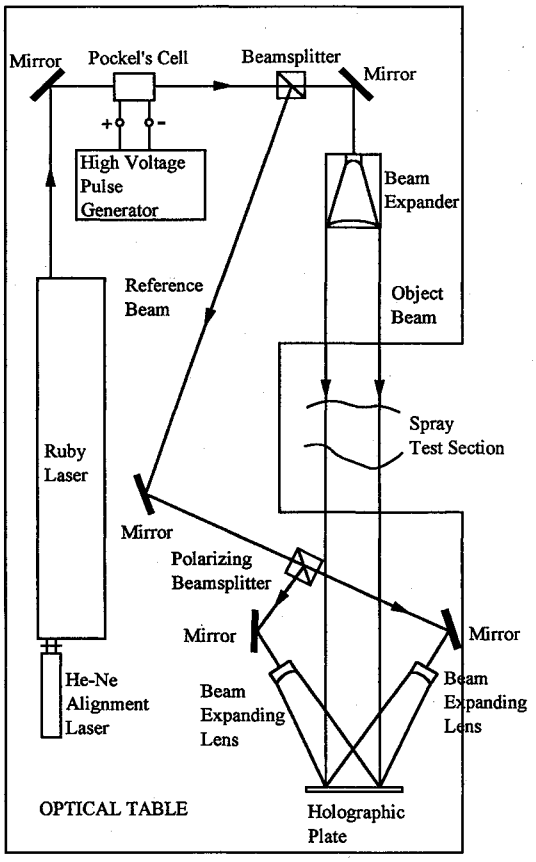

Fig. 2 Schematic of the optical setup for double-pulse holography with two reference beams.

A Pockels Cell was used to change the polarization direction of the first pulse. To drive the Pockels Cell, a high-voltage pulse generator was employed. The input signal to this device comes from a synchronization socket in the ruby laser control box. To change the polarization direction of the first pulse only, the Pockels Cell was activated just before the first pulse throughout the duration of the first pulse. To this end, the high-voltage pulse generator provides an adjustable input/output delay and pulse width, from 0.2 to 1.2 ms and from 40 to 1.2 ms, respectively. The output pulse amplitude ranges from 2.0 to 7.5 kV.

A beam-splitter divided the incoming laser beam into an object beam and a reference beam. The object beam was expanded and collimated by a Galilean-type beam expander. The diameter of the object beam was increased up to 0.1 m to cover entirely the spray region of interest. This plane wave passed through the spray region and finally was intercepted at the 0.10 $\times$ 0.13 m holographic glass plate.

The reference beam passed through a cube-type polarization beam-splitter. This beam-splitter reflected the vertical components of polarization in the incident light while permitting the horizontal components to pass undeviated. Therefore, the reference beam of the first pulse, whose polarization direction was changed horizontally by the Pockels Cell, passed through the beam-splitter without any change of direction. The reference beam of the second pulse was reflected at the diagonal plane in the beam-splitter. In this manner, two reference beams that had different incident angles interfered with the object wave. This produced two separate holograms, each corresponding to a laser pulse. Each reference wave was diverged

Table 1 Summary of test conditions

Case	Liquid	D_j, mm	2θ, deg	V_j, m/s	Re_j	We_j
H1-1	Water	1.016	90	12.0	8,590	1,000
H1-2	Water	1.016	90	12.0	8,590	1,000
H1-3	Water	1.016	90	12.0	8,590	1,000
H2	Water	1.016	60	12.0	6,070	500
H3	Water	1.016	120	12.0	10,520	1,500
H4	Water	1.016	90	15.4	11,020	1,650
H5	Water	1.016	90	19.1	13,670	2,540
H6	Water	1.534	90	11.9	12,860	1,490
E1	Ethanol	1.016	90	7.2	3,410	920
E2	Ethanol	1.016	90	9.1	4,300	1,460
E3	Ethanol	1.016	90	11.9	5,640	2,520
G1	50% glycerol	1.016	90	8.0	1,070	530
G2	59% glycerol	1.016	90	12.3	990	1,290
G3	68% glycerol	1.016	90	11.7	510	1,210

by a plano-concave lens to cover the entire holographic plate. Neutral density filters were used to control the reference-to-object-beam ratio as well as the total irradiance at the holographic plate to improve the quality of the holograms. The entire setup was placed on a vibration-isolation optical table.

To find the magnification factor and locate the droplet position, one more hologram of the grid object was taken after fabricating a spray hologram, without any changes in the optical system. The grid with numbered horizontal and vertical lines at 5.0-mm intervals was drawn by a computer, copied onto transparent paper, and attached to a transparent glass plate.

C. Hologram Reconstruction and Image Processing System

The holograms were reconstructed using a 10-mW He–Ne laser. The reconstructed virtual image of the spray was magnified by a Questar telescope macrolens system. A camera, attached to the end of this system, recorded the magnified microscopic images of the liquid droplets. Six different locations were identified and studied for both pulses, i.e., three locations in the horizontal direction with $\Delta x = \pm 25$ mm from the spray axis, at two locations ($\Delta y = 25$ mm) on the spray axis. The sampling area at each location was approximately (Δx, Δy) = (10×15 mm). At one location the droplet images and the grid were photographed. The droplet images were magnified seven times in the final photographic print (75×110 mm). The results on the droplet diameters and velocities presented in this article were obtained after averaging the measurements in the previous six locations (unless otherwise noted).

The images of droplets and grids printed on the photographic papers were captured by a charge-coupled device camera and inputted into a personal computer for the image analysis. Image Analyst provided by Automatrix, Inc. was used as the image processing software. The magnification factor between the length of the image on the monitor and the actual length of the image was calculated by measuring the length of one grid, the real distance of which is 5.0 mm. The value of the conversion factor in this study ranges from 24.3 to 27.9 μm per one pixel of the monitor. The diameters of droplets were obtained by measuring the total area of droplets and calculating the equivalent diameter of a circle corresponding to the total area.

To measure the horizontal and vertical velocities of droplets, the absolute coordinates of the centroid of the droplets from the origin of the grid for both pulses were measured. Next, the difference in the coordinates of the centroid in each direction between two pulses was divided by the pulse separation time. To verify the accuracy of the diameter measurements, the holograms of a 4.763-mm precision steel ball and a 306.6-μm steel wire were fabricated. The diameters of the steel ball and the wire were measured in the same manner as described for the measurements of the liquid droplet diameters. The relative error between the ball size and the holographic measurement of the diameter was within 5%. The approximate error involved in the velocity measurements of droplets was estimated in the following manner. Assuming a maximum of 4 pixels of error (this value is arbitrary, but reasonable, for the maximum value based on experience) in the distance measurements, the corresponding error in distance is 111.6 μm using the maximum conversion ratio (27.9 μm/pixel). The error in velocity for this distance is 2.2 m/s with 50-μs pulse separation time. This value is within 20% of measured velocities of droplets for $V_j = 12.0$ m/s.

Table 2 Physical properties of the liquids used in the experiment at 20°C and 1 atm

Liquid	Density, kg/m^3	Viscosity $\times 10^3$, N s/m^2	Surface tension $\times 10^3$, N/m
Water	998 (1.0)	1.002 (1.0)	72.88 (1.0)
Ethanol	791 (0.79)	1.200 (1.20)	22.80 (0.31)
50% glycerol	1124.9 (1.13)	6.05 (6.04)	69.68 (0.96)
59% glycerol	1149.5 (1.15)	10.25 (10.23)	68.70 (0.94)
68% glycerol	1174.2 (1.18)	19.40 (19.36)	67.72 (0.93)

The total number of droplets measured for each test condition ranged between 500–1000. This is a relatively small sample size compared to the recommended value (5500) (Ref. 15). However, this is inevitable because the measurements were made from the instantaneous spray images (for 30 ns) rather than collecting a large amount of data over a time period (e.g., a couple of seconds as is customarily done with other laser instruments). Processing of the data is very tedious because the data-analysis procedure for the droplet size and velocity measurements is not currently automated.

D. Test Conditions and Physical Properties of Liquid

The test conditions are summarized in Table 1. The Reynolds and Weber numbers of the liquid jet are based on the orifice diameter, liquid properties, and horizontal component of the liquid jet velocity ($V_j \sin \theta$). The reason for electing to use the horizontal component of the jet velocity instead of the jet velocity in itself is twofold: first, the horizontal momentum of each liquid jet is closely related to the liquid sheet spreading and atomization; second, this choice allows for the effect of the impingement angle to be reflected in the definition of Re_j and We_j when the jet velocity is kept constant.

The effect of the impingement angle, liquid jet velocity, and orifice diameter was examined in the series H of experiments with water. The condition for experiment H1 ($D_j = 1.016$ mm, $2\theta = 90$ deg, and $V_j = 12.0$ m/s) is considered as the baseline condition. Three experiments with the baseline condition were performed to verify the repeatability of the experimental results. The effect of liquid properties on the spray characteristics was investigated with ethanol (E series) and three glycerol solutions (G series). The mixing percentage of glycerol solutions is by mass throughout this study. The physical properties of the liquids used in the experiments at 20°C and 1 atm are

shown in Table 2. The values in parentheses represent the ratio of the properties of ethanol and glycerol to the properties of water.

III. Results

A. Overall Spray Pattern

Visual observations indicated that the generated sprays with the liquid jet velocities up to 12 m/s were primarily two dimensional (fan spray). However, they became three dimensional (cone spray) when the liquid jet velocities exceeded 15 m/s. Because of space limitations, no photographs of the overall spray pattern are shown. A considerable amount of additional information can be found in Ref. 16. Instead, a description of the phenomena observed will be presented. Generally, a small fan-shaped liquid sheet formed near the impingement point caused by the obliquely colliding high-speed jets. Circumferentially aligned liquid ligaments detached directly from this liquid sheet. These ligaments progressively broke up into droplets as they moved downstream. The expanding angle of the liquid sheet and arc-shaped liquid ligaments greatly increased with an increase in the impingement angle. At the lowest impingement angle, $2\theta = 60$ deg, the size of droplets was noticeably larger than that for the higher impingement angles. This is because the size of liquid ligaments, which break up into droplets, is larger at this condition. Increasing the impingement velocity did not substantially alter the overall spray pattern. However, smaller droplets were produced with an increase of the liquid jet velocity, as will be shown quantitatively in the next section. The shape and size of the liquid sheet were also very irregular and smaller for higher velocities compared to low jet velocities. An increase of the orifice diameter from $D_j = 1.016$ to 1.534 mm, with $V_j = 12.0$ m/s, $2\theta = 90$ deg, generated an entirely different spray pattern. The liquid sheet around the impingement point became larger and large liquid ligaments existed in the far downstream region of the spray.

The effect of liquid properties on the overall spray pattern was studied for $D_j = 1.016$ mm, $2\theta = 90$ deg. The viscosity of ethanol does not change much compared to that of water. However, the surface tension of ethanol is 30% that of water. In general, the surface tension of liquid represents the resisting force for the formation of the new surface area. This implies that liquid with lower surface tension is easier to disintegrate. No pronounced effect of surface tension on the overall spray pattern was observed. This fact is also confirmed by Heidmann et al.[4] using Varsol, the surface tension of which was reduced to about one-half that of water. However, the effect of surface tension is more evident in the droplet size (the mean droplet diameters of the ethanol spray were found to be much smaller than those of the water spray, as will be discussed in the next section).

The viscosity of liquid plays an important role in many aspects of atomization. An increase in viscosity lowers the Reynolds number and also prevents the progress of any natural instabilities. These instabilities in the jets and sheets are the main impetus for the atomization of liquid. Therefore, the combined effect of an increase in viscosity is to delay disintegration and increase the size of droplets in the spray. Experiments with glycerol solution (Table 2) featured arc-shaped liquid ligaments detaching earlier from the liquid sheet near the impingement point and stretching out further downstream in the spray. This is attributed to the delay of the breakup of ligaments because of the high viscosity of glycerol.

B. Droplet Size Measurements

Figure 3 shows typical photographs of droplet images at the first and second pulses, which are used for the measurements of droplet size and velocity. The droplet diameters were obtained by measuring the total area of each droplet and calculating the equivalent diameter of a circle corresponding to that area. This figure demonstrates the ability of the double-pulse holographic technique to record the size and position of liquid elements at two different times. The region shown is downstream along the spray axis. The movement of droplets can be clearly seen and the identification of the same droplets between the two photographs is not difficult. For example, the droplet identified as no. 1 in Fig. 3a, corresponding to the first pulse, moved to the location identified as no. 1 in Fig. 3b, corresponding to the second pulse. The benefit from the separation of the first and second droplet images is remarkable. In conventional double-pulse holography, the droplet images in Fig. 3b would overlap with the images in Fig. 3a. This photograph also demonstrates the size diversity of the liquid elements as well as the fact that these elements are largely nonspherical.

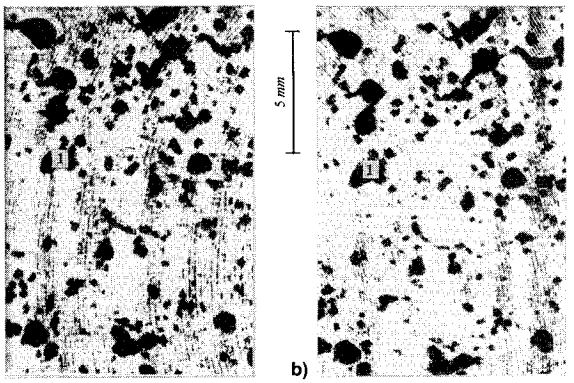

Fig. 3 Photographs of hologram revealing droplet images at the first and the second pulse with $D_j = 1.016$ mm, $2\theta = 60$ deg, $V_j = 12.0$ m/s, $(x, y) = (0.0$ cm, 4.0 cm). Droplet images at the a) first pulse and b) second pulse.

To check the repeatability of the experimental results, preliminary experiments were conducted. Three experiments with the baseline condition ($D_j = 1.016$ mm, $2\theta = 90$ deg, and $V_j = 12.0$ m/s) were performed for this purpose. The maximum changes in mean droplet diameters with respect to the averaged mean diameters for three runs are within 6% for D_{10} and 15% for D_{32}. Here, D_{10} and D_{32} are length- and Sauter-mean diameters. Based on the previous results, it is confirmed that the measurement results for mean droplet diameters are within allowable repeatability.

The effect of the impingement angle, liquid jet velocity, and orifice diameter on the droplet diameter is shown in Fig. 4. D_{MMD}(mass median diameter) is the drop size for which the masses in drops larger and smaller than this diameter are equal. In an average sense, smaller droplets (desirable from the combustion standpoint) are produced with larger impingement angles, higher jet velocities, and smaller orifice diameters. As the impingement angle and liquid jet velocity are increased, the horizontal momentum of the liquid jet is increased, resulting in the increase of the horizontal impact force between two liquid jets. Therefore, the liquid is more widely dispersed, centering around the impingement point. Consequently, the thickness of the liquid sheet and liquid ligaments decreases, resulting in smaller droplets. An increase of the orifice diameter from $D_j = 1.016$ to 1.534 mm produced a spray characterized by large liquid ligaments in the far downstream region of the spray. Relatively large-size droplets are produced by the breakup of these ligaments or by direct detachment of liquid from the boundary of ligaments.

Figure 5 shows the effect of liquid properties on the droplet diameter for $D_j = 1.016$ mm, $2\theta = 90$ deg. The mean diameters of water and three glycerol solutions fall almost in a straight line, regardless of the fact that these data represent the variation of liquid viscosity up to 20 times the viscosity of water. This finding is interesting because the spray pattern of the glycerol solutions was visibly different from that of water at the same liquid jet velocity. On the other hand, the mean diameters of the ethanol spray always fall in the lower region

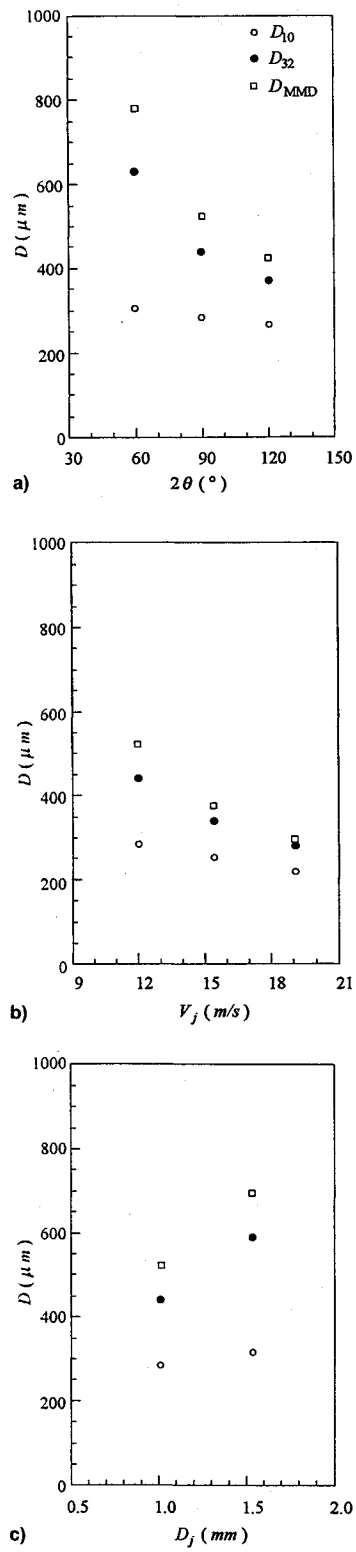

Fig. 4 Effect of the impingement angle, liquid jet velocity, and orifice diameter on mean diameters: a) D_j = 1.016 mm, V_j = 12.0 m/s, b) D_j = 1.016 mm, 2θ = 90 deg, and c) V_j = 12.0 m/s, 2θ = 90 deg. The maximum relative error in the measurements was 5%.

of the previously mentioned straight line, even though there was no big difference in the overall spray patterns of ethanol and water. Based on the previous findings, it can be concluded that the surface tension of the liquid plays an important role on the droplet size of the spray without noticeable change in the overall spray pattern, whereas viscosity affects the overall spray pattern without marked effects on the droplet size of the spray.

The present results for the droplet diameters were compared with existing available results in Fig. 6. The orifice diameter used in the comparison for the present study is 1.016 and those for Heidmann and Foster,[6] Dombrowski and Hooper,[7] and Anderson et al.[9] are 2.26, 0.5, and 0.64, respectively. Only the comparisons with the most recent of these studies are shown in Fig. 6, for brevity. Generally, the results with the larger orifice diameter featured larger droplet sizes (Fig. 6). A decrease of the droplet diameters with an increase of the impingement angle and liquid jet velocity was observed in all of the results of other researchers,[6,7,9] which is in agreement with the trends of the present study.

C. Droplet Size Distribution

Numerous attempts have been made to obtain suitable mathematical or empirical expressions for the drop-size distribution

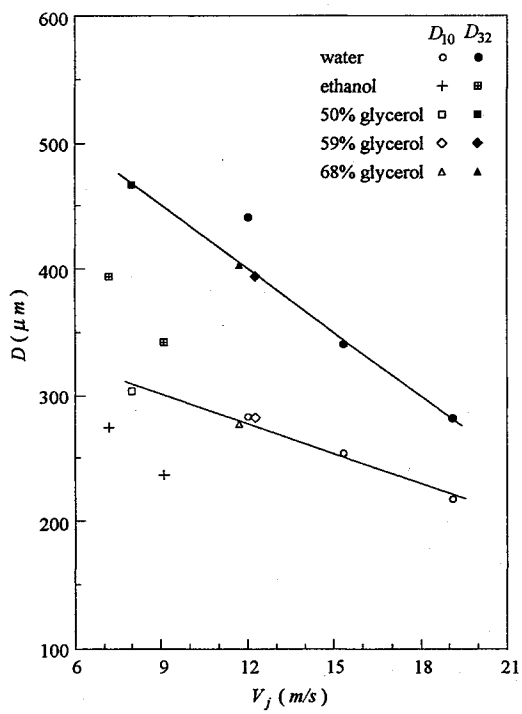

Fig. 5 Effect of liquid properties on mean diameters for D_j = 1.016 mm, 2θ = 90 deg. The maximum relative error in the measurements was 5%.

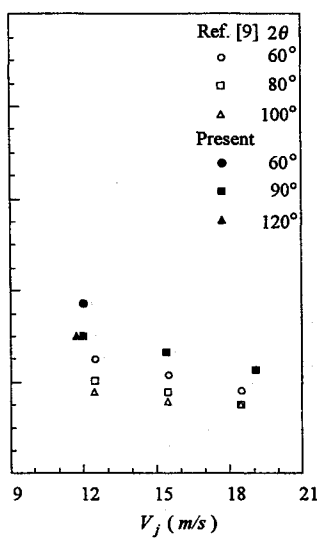

Fig. 6 Comparison of the size measurement results (D_j = 1.016 mm) with D_{10} results from Anderson et al.[9] for D_j = 0.64 mm.

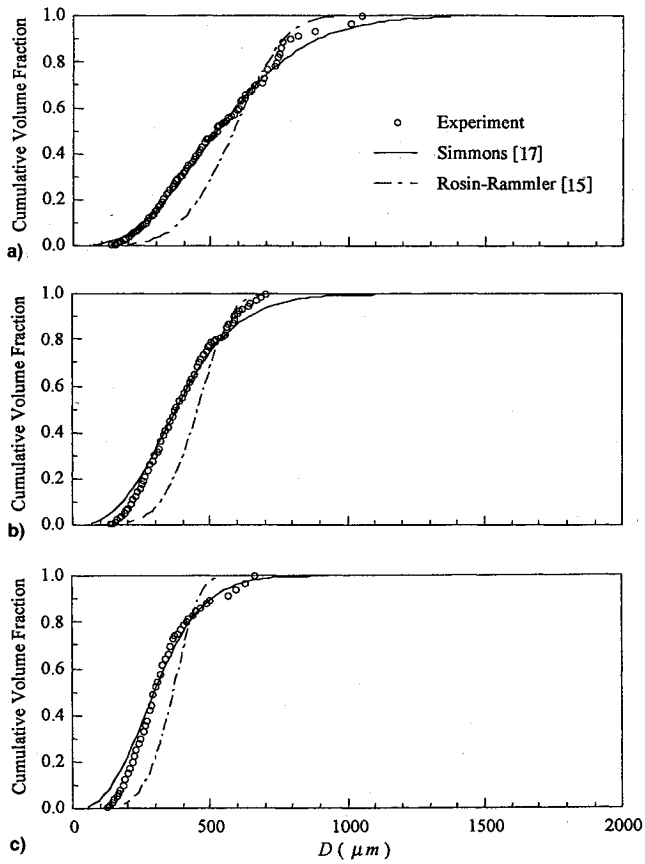

Fig. 7 Comparison of cumulative volume distributions with the Simmons and Rossin–Rammler distributions for water, D_j = 1.016 mm, 2θ = 90 deg. V_j = a) 12.0, b) 15.4, and c) 19.1 m/s.

in sprays. Those in general use include the normal, log-normal, Nukiyama–Tanasawa, Rosin–Rammler, and upper-limit distributions.[15] In the present study, the Rosin–Rammler distribution, which is one of the most widely used expressions presently, and the universal root-normal distribution proposed by Simmons[17] were compared with experimental data.

The universal root-normal and Rosin–Rammler distributions are compared with the experimental results in Figs. 7 and 8. In most of the cases, the superiority of the universal root-normal distribution to the Rosin–Rammler distribution is obvious. The effect of jet velocity on the cumulative volume distribution is shown in Fig. 7. The maximum diameter and the slope of the curve changes noticeably when the jet velocity changes from V_j = 12.0 to 15.4 m/s. No substantial variation is observed once the liquid jet velocity is over 15.0 m/s. The slope of the curve becomes steeper as the jet velocity is increased. This implies that the droplet diameters that have the same percentage of total liquid volume become smaller. For example, the D_{MMD} (50% of total liquid volume is within this diameter) obtained from the experimental data is 523.41, 375.31, and 295.35 μm for V_j = 12.0, 15.4, and 19.1 m/s, respectively. The cumulative volume distributions for different liquids shown in Fig. 8 feature slopes that are a bit steeper than that of water at similar operating conditions.

D. Droplet Velocity Measurement

The effects of the impingement angle, liquid jet velocity, and orifice diameter on the droplet velocities were also investigated. Only the results of the liquid jet velocity are shown in Fig. 9 because of space limitations. Additional information can be found in Ref. 16. In an average sense, faster droplets are generated with larger impingement angle, higher jet velocity, and smaller orifice diameter. The droplet velocities are almost linearly proportional to the liquid jet velocity as shown in Fig. 9. The magnitude of the droplet velocities is similar to that of the liquid jet velocity, which implies that the velocities of other liquid elements (liquid sheet or liquid ligaments) are also close to the liquid jet velocity. The horizontal velocities did not change markedly by varying the primary parameters, whereas the vertical velocities show the same trend as the mean droplet velocities.

Figure 10 shows the effect of liquid properties on the droplet velocities for D_j = 1.016 mm and 2θ = 90 deg. The linear

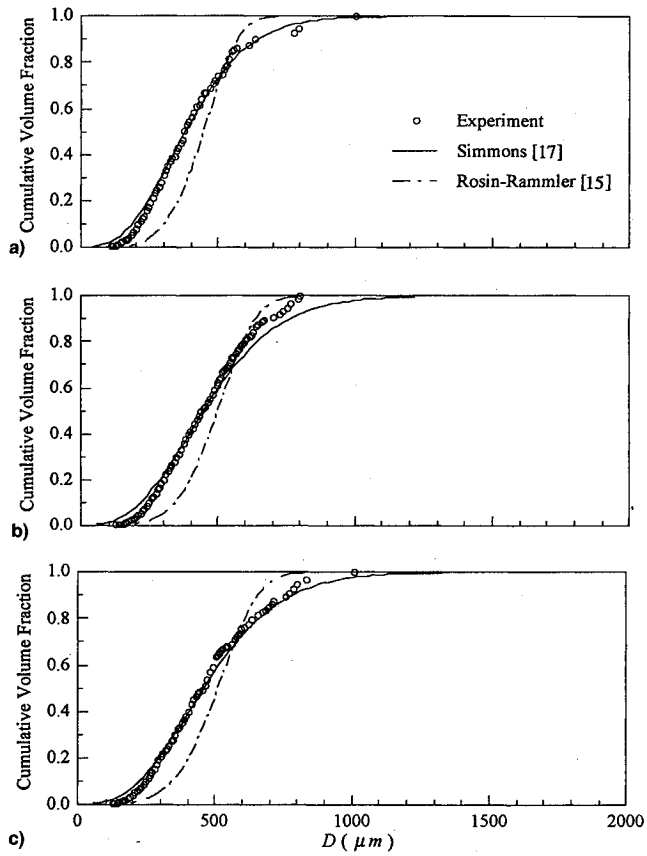

Fig. 8 Comparison of cumulative volume distributions with the Simmons and Rossin–Rammler distributions for D_j = 1.016 mm, 2θ = 90 deg: a) ethanol, V_j = 11.9 m/s; b) glycerol (59%), V_j = 12.3 m/s; and c) glycerol (68%), V_j = 11.7 m/s.

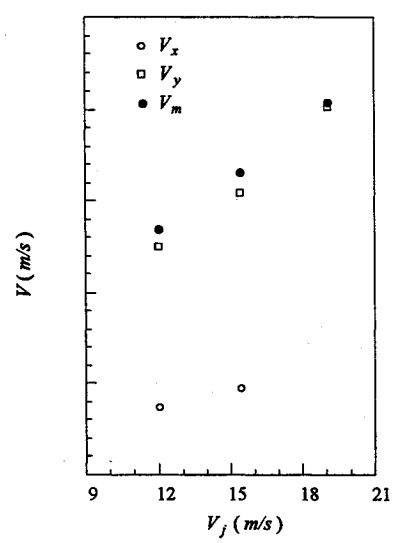

Fig. 9 Effect of the liquid jet velocity on mean velocities D_j = 1.016 mm, 2θ = 90 deg. The maximum relative error in the measurements was 20%.

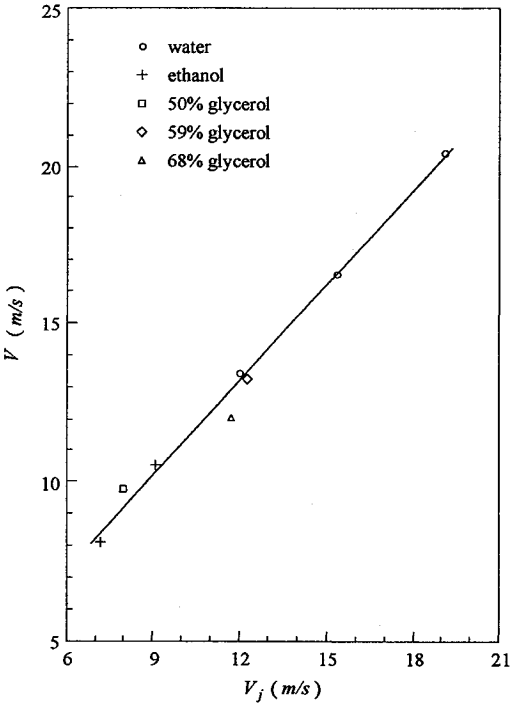

Fig. 10 Effect of liquid properties on mean velocities for D_j = 1.016 mm, 2θ = 90 deg. The maximum relative error in the measurements was 20%.

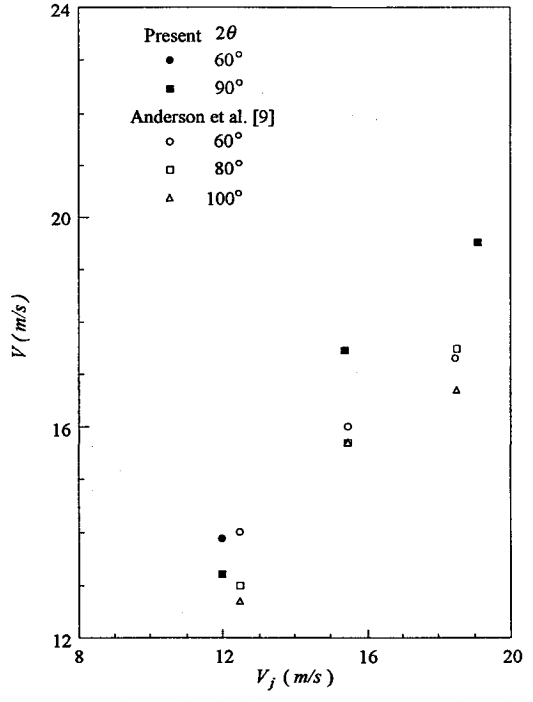

Fig. 11 Comparison of velocity measurement results with those of Anderson et al.[9] (D_j = 1.016 and 0.64 mm for the present study and Anderson et al.,[9] respectively.)

proportionality of the droplet velocities to the liquid jet velocity (already shown in Fig. 9) is still apparent in spite of the large variation in the physical properties of the liquid (surface tension and viscosity). According to this observation, we can conclude that, in the parametric domain studied, the physical properties of the liquid do not markedly affect the droplet velocities of the resulting spray, whereas they have an effect on the droplet diameters, as discussed earlier.

Limited experimental data are available for the comparison of measurements of droplet velocities. Figure 11 shows a comparison of the results of the present velocity measurements with those of Anderson et al.[9] Note that the orifice diameter they used is smaller (D_j = 0.64 mm) than that of the present study (D_j = 1.016 mm) and the position they probed was y = 41 mm at the spray axis, while the present results in Fig. 11 were taken from the region y = 50 to 70 mm at the spray axis (x = 0). The velocities in Ref. 9 are generally smaller than those of the present study. The trends agree rather well.

IV. Conclusions

In this article an experimental study of the fluid dynamics of a spray created by two impinging jets was presented. The experiments with two nonevaporating impinging jets injected into still air at atmospheric pressure were conducted utilizing a novel two-reference-beam double-pulse holographic technique. This holographic method features the capability of separation of the first and second droplet images by using two reference beams and polarization of the laser light. The effect of the impingement angle, liquid jet velocity, orifice diameter, and liquid properties on the atomization process was investigated using water, ethanol, and three glycerol solutions. Visualization of the structure of the generated spray as well as measurements on the size and velocity of the liquid droplets were performed.

The results confirmed the inherent wave nature in the disintegration process characteristic of this kind of atomization. This feature was more distinct with high-viscosity liquids. The overall spray pattern was mainly affected by the impingement angle, orifice diameter, and viscosity of liquid, whereas the liquid jet velocity and the surface tension of the liquid had no significant effect.

Smaller and faster droplets were generated with larger impingement angle, higher jet velocity, and smaller orifice diameter. The relative error in the droplet diameter measurements was 5% and in the velocity measurements 20%. The surface tension of the liquid plays an important role in the droplet size of the spray without any noticeable change in the overall spray pattern. Viscosity affects the structure of the spray without significant effects on the droplet size. It was also found that the liquid properties did not markedly affect the droplet velocities. The superiority of the universal root-normal droplet size distribution to the Rosin–Rammler distribution was proved in the great majority of tested cases.

Acknowledgments

The support of the U.S. Air Force Office of Scientific Research under Grant AFOSR F49620-92-J-0343 is gratefully acknowledged. We thank G. M. Faeth of the University of Michigan for his recommendation that we compare our droplet size measurements to the Simmons correlation.

References

[1]Sutton, G. P., *Rocket Propulsion Element: An Introduction to the Engineering of Rockets*, Wiley, New York, 1992.

[2]Harrje, D. T., and Reardon, F. H., *Liquid Propellant Rocket Combustion Instability*, NASA SP-194, 1972.

[3]Heidmann, M. F., and Humphrey, J. C., "Fluctuations in a Spray Formed by Two Impinging Jets," NACA TN 2349, 1951.

[4]Heidmann, M. F., Priem, R. J., and Humphrey, J. C., "A Study of Sprays Formed by Two Impinging Jets," NACA TN 3835, 1957.

[5]Foster, H. H., and Heidmann, M. F., "Spatial Characteristics of a Water Spray Formed by Two Impinging Jets at Several Jet Velocities in Quiescent Air," NASA TN D-301, 1960.

[6]Heidmann, M. F., and Foster, H. H., "Effect of Impingement Angle on Drop Size Distribution and Spray Pattern of Two Impinging Water Jets," NASA TN D-872, 1961.

[7]Dombrowski, N., and Hooper, P. C., "A Study of the Sprays Formed by Impinging Jets in Laminar and Turbulent Flow," *Journal of Fluid Mechanics*, Vol. 18, 1963, p. 392.

[8]Huang, J. C. P., "The Break-up of Axisymmetric Liquid Sheets,"

Journal of Fluid Mechanics, Vol. 43, 1970, p. 305.

[9]Anderson, W. E., Ryan, H. M., Pal, S., and Santoro, R. J., "Fundamental Studies of Impinging Liquid Jets," AIAA Paper 92-0458, 1992.

[10]Dombrowski, N., and Johns, W. R., "The Aerodynamic Instability and Disintegration of Viscous Liquid Sheets," *Chemical Engineering Science*, Vol. 18, 1963, p. 203.

[11]Ryan, H. M., Anderson, W. E., Pal, S., and Santoro, R. J., "Atomization Characteristics of Impinging Liquid Jets," *Journal of Propulsion and Power*, Vol. 11, No. 1, 1995, pp. 135–145.

[12]Ibrahim, E. A., and Przekwas, A. J., "Impinging Jets Atomization," *Physics of Fluids A*, Vol. 3, 1991, p. 2981.

[13]Vassallo, P., and Ashgriz, N., "Effect of Flow Rate on the Spray Characteristics of Impinging Water Jets," *Journal of Propulsion and Power*, Vol. 8, 1992, p. 980.

[14]Kang, B., Poulikakos, D., and Shen, Y., "Holography Experiments on Impinging Liquid Jet Atomization: Testing of Theoretical Predictions," *Atomization and Sprays*, Vol. 5, 1995, pp. 387–402.

[15]Lefebvre, A. H., *Atomization and Sprays*, Hemisphere, New York, 1989.

[16]Kang, B., "A Holographic Study of the Dense Region of a Spray Created by Two Impinging Jets,"Ph.D. Dissertation, Univ. of Illinois at Chicago, IL, 1995.

[17]Simmons, H. C., "The Correlation of Drop-Size Distributions in Fuel Nozzle Sprays," *Journal of Engineering for Power*, Vol. 99, No. 3, 1977, pp. 309–317.